



Contents lists available at ScienceDirect

International Journal of Solids and Structures

journal homepage: www.elsevier.com/locate/ijsolstr

The interfacial analysis of a film bonded to a finite thickness graded substrate

Peijian Chen, Juan Peng*, Liyuan Yu, Yugui Yang

State Key Laboratory for Geomechanics and Deep Underground Engineering, School of Mechanics and Civil Engineering, School of Physics, China University of Mining and Technology, Xuzhou, Jiangsu, 221116, China

ARTICLE INFO

Article history:

Received 7 December 2016

Revised 10 April 2017

Available online xxx

Keywords:

Bonded problem

Loading condition

Stress intensity factor

Film/substrate system

ABSTRACT

The problem of an elastic film bonded to a finite-thickness graded substrate under different loading conditions is investigated, in which the shear modulus of the graded substrate is assumed to vary exponentially along its thickness and perfect adhesion is adopted at the contact interface. The governing singular integral equation for the present model is formulated analytically in terms of interfacial shear stress. With the help of the collocation method, the governing equation is further solved numerically. The interfacial shear stress, the normal stress in the film as well as the singularity near the film edges are discussed in order to evaluate the interface behaviors that are closely related to failure and destruction of the film/substrate systems. It is found that the interface behavior of the film/substrate system can be modified by tuning the material and geometric parameters of both the film and the graded substrate. Compared with cases under a non-symmetric loading and a symmetric one, the effect of some parameters is observed to be dependent of the loading type.

© 2017 Elsevier Ltd. All rights reserved.

1. Introduction

The mechanical behavior of film/substrate systems are of interest in a wide range of industrial, hi-tech and biotechnological applications in recent decades, including, for example, piezoelectric sensors and actuators attached to a structure to monitor and control the deformation and vibration of the host structure (Fang et al., 2013; Gladwell, 1980; Jin and Wang, 2011), stretchable and flexible electronics made of inorganic films and soft substrate (Dai et al., 2015), and etc. A film/substrate system can also be used to uncover the mechanism of cell differentiations, which are affected by the surrounding substrate (Banerjee and Marchetti, 2012). The challenge of establishing suitable models is therefore constantly faced to predict the interface stresses that may result in failure and destruction of the film/substrate systems (Huang et al., 2010).

Various studies have been done to access the interface stress distribution in the film/substrate system. Generally, these works can be categorized into two typical approaches. The first one, represented by Akisanya and Fleck (1994) and Yu et al. (2001), makes an assumption that a pre-existing crack lies on the edge of a thin film, and deals the problem with the fracture mechanics theory. Nevertheless, a lack of pre-existing cracks or defects would be cru-

cial in many cases (Hu, 1979). The second one could be termed as a contact model, in which perfect bonding between the film and the corresponding substrate is assumed and contact mechanics is used to find the stress field at the interface and near the edge of the film. Using a contact model, Arutiunian (1968) studied the contact problem between a half plane and a stiffener with finite length, and gave an infinite power series solution. The same problem was well solved by Erdogan and Gupta (1971) later through tackling the governing singular integral equation into terms of the interface shear stress. Shield and Kim (1992), considering the bending stiffness of the film, employed a beam theory model for a thin film bonded to an elastic half plane to incorporate normal stresses at contact interface to the interfacial shear ones. The multi-layered films or multi-periodic films bonded to an elastic substrate was modeled by Erodgan and Joseph (1990a,b). A closed form solution of the governing singular equation was obtained by Alaca et al. (2002) by adopting Vekua's solution procedure of Prandtl's equation and assuming a nearly rectangular film profile. Jin and Wang (2011) discussed the electromechanical behavior of surface-bonded piezoelectric film attached to an infinite elastic half plane including the adhesive layer. Analysis of stress singularity in thin film bonded structures is considered by Lanzoni (2011) for several geometric configurations under different loading conditions. Recently, the problem of a Timoshenko beam of finite length perfectly bonded to a homogeneous isotropic half plane loaded by

* Corresponding author.

E-mail addresses: chenpeijian@cumt.edu.cn (P. Chen), pengjuan@cumt.edu.cn (J. Peng).

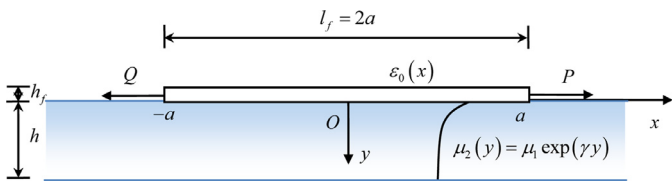


Fig. 1. The two-dimensional non-slipping contact model between an elastic film of length l_f and a finite-thickness graded substrate. h is the length of the graded substrate.

concentrated forces and couples is considered by Lanzoni and Radi (2016).

All the bonded models mentioned above involve homogeneous materials. Materials with gradient variation along certain direction have been widely found in nature, for example, teeth and bones (Suresh, 2001). What is more, functionally graded materials (FGM) have attracted numerous attentions of scientists due to their novel performance (Giannakopoulos and Pallot, 2000; Qian et al., 2009) in various present and potential applications. The traditional contact problem between a stamp or punch and a graded medium have been explored extensively to find the contact stress that would cause crack initiation of wear of surface. These works include Booker et al. (1985), Guler and Erdogan (2004, 2007), Choi and Paulino (2008, 2010), Ke and his co-workers (2006, 2008), El-loumi et al. (2010), Chen and Chen (2013a,b), Dag et al. (2012), Chen et al. (2015), Jin et al. (2013), etc. In the mentioned works, contact stresses at the contact region are mainly focused. As for the sub-surface stresses and local deflection of a graded medium loaded by a pre-determined pressure or a rigid punch, Chidlow et al. (2011, 2012) proposed a valid analytical method.

Although both experimental studies and theoretical researches on the contact mechanics of graded materials have been reported, existing literature is mainly concerned with the traditional indentation problem, and few works have discussed the bonded problem between a deformable layer and a graded medium. Guler (2008) and Guler et al. (2012) explored the contact problem between a thin film and a graded/FGM coated half plane using both FEM and analytical methods. Recently, Chen et al., (2016a, b) investigated the contact problem of an elastic film subjected to a mismatch strain on a finite-thickness graded substrate. It was found that the interfacial behavior is significantly influenced by the thickness of the graded substrate. Whether the result under a mismatch strain loading condition is consistent with that under a non-symmetric load when a film bonded to a finite-thickness graded substrate? How can we tune different material and geometric parameters to improve the interfacial behavior?

In order to answer the above questions, a non-slipping contact model is established in this paper, in which an elastic film attach to a graded substrate of finite thickness under a non-symmetric loading condition. The governing integro-differential equation for the present model is formulated analytically in terms of interfacial shear stress, and is further solved numerically with the help of the collocation method. The interfacial shear stress, the normal stress in the film as well as the singularity near the film edges are mainly discussed in order to evaluate the interface behavior that is closely related to failure and destruction of the film/substrate systems

2. The bonded model of a thin film on a finite-thickness graded substrate

The two-dimensional non-slipping contact model between an elastic film and a finite-thickness graded substrate which is fixed on a rigid foundation is shown in Fig. 1, where the length of the film is $l_f=2a$. h_f , μ_f , ν_f are denoted as the thickness, the shear

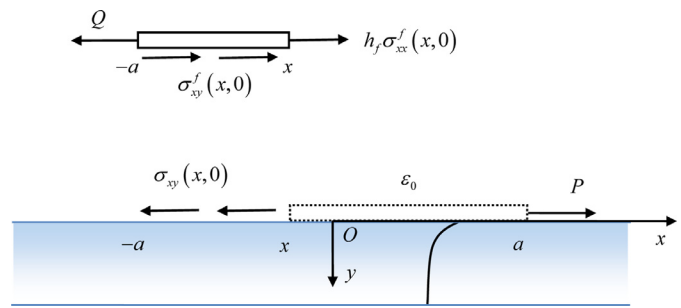


Fig. 2. Schematic of the mechanical behavior of the bonded interface between a film and an elastically graded substrate.

modulus and the Poisson's ratio of the film, respectively, and h is the thickness of the graded substrate.

The shear modulus of the graded substrate is assumed to abide by

$$\mu_2(y) = \mu_1 \exp(\gamma y), \quad 0 \leq y \leq h, \quad (1)$$

where μ_1 is the value of shear modulus at the surface of the graded substrate. γ is a constant characterizing the inhomogeneity of material, which can be expressed as

$$\gamma = \frac{1}{h} \ln \left(\frac{\mu_3}{\mu_1} \right). \quad (2)$$

where μ_3 corresponds to the shear modulus at the bottom of the graded substrate. The exponential function is commonly used to describe a graded medium in existing theoretical models, and it covers a fairly broad class of graded materials, for example, graded γ -TiAl/Y-TZP and Ni- Al_2O_3 (Suresh, 2001; Suresh et al., 1997). When $\gamma=0$ is chosen, the finite-thickness graded substrate will reduced to a homogeneous elastic one. Note that the problem of a thin-film bonded to an elastic layer subjected to a thermal variation has been well solved by Lanzoni and Radi (2009). In the present model, the Poisson's ratio of the graded substrate is assumed to be a constant ν due to the neglectable effect.

3. Governing equation of the present model

For the present plane contact problem, the equilibrium equations of the graded substrate in absence of body forces can be written as (Chen et al., 2016b),

$$\begin{aligned} (\kappa + 1) \frac{\partial^2 u}{\partial x^2} + 2 \frac{\partial^2 v}{\partial x \partial y} + (\kappa - 1) \frac{\partial^2 u}{\partial y^2} + \gamma(\kappa - 1) \frac{\partial u}{\partial y} \\ + \gamma(\kappa - 1) \frac{\partial v}{\partial x} = 0, \end{aligned} \quad (3)$$

$$\begin{aligned} (\kappa - 1) \frac{\partial^2 v}{\partial x^2} + 2 \frac{\partial^2 u}{\partial x \partial y} + (\kappa + 1) \frac{\partial^2 v}{\partial y^2} + \gamma(3 - \kappa) \frac{\partial u}{\partial x} \\ + \gamma(\kappa + 1) \frac{\partial v}{\partial y} = 0, \end{aligned} \quad (4)$$

where $u(x, y)$ and $v(x, y)$ are the displacement components in x and y directions, respectively, $\kappa = 3 - 4\nu$ is adopted for the plane strain case and $\kappa = (3 - \nu)/(1 + \nu)$ for the plane stress one.

Taking the Fourier transform of Eqs. (3) and (4), and carrying out a lengthy mathematic analysis similar to Chen and Chen (2013b), the surface displacements of the graded substrate $u(x, 0)$ and $v(x, 0)$ can be expressed as

$$\begin{aligned} \frac{\partial u(x, 0)}{\partial x} = -\frac{\kappa + 1}{4\pi\mu_1} \int_{-a}^a \frac{\sigma_{xy}(r, 0)}{r - x} dr + \frac{\kappa - 1}{4\mu_1} \sigma_{yy}(x, 0) \\ + \frac{1}{\pi} \int_{-a}^a [K_{11}(x, r) \sigma_{xy}(r, 0) + K_{12}(x, r) \sigma_{yy}(r, 0)] dr. \end{aligned} \quad (5)$$

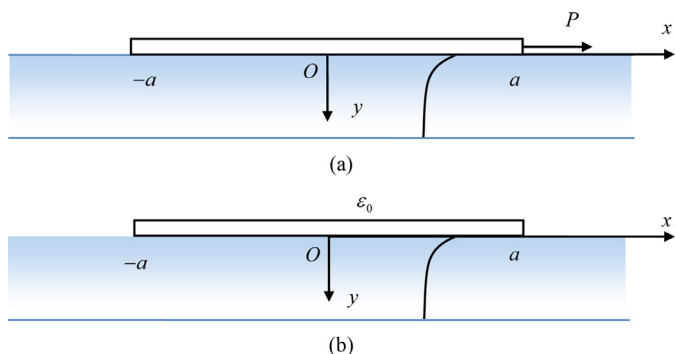


Fig. 3. (a) The bonded model between an elastic film and a graded substrate under a loading at a single end on the film; (b) The model under a mismatch strain loading at the interface.

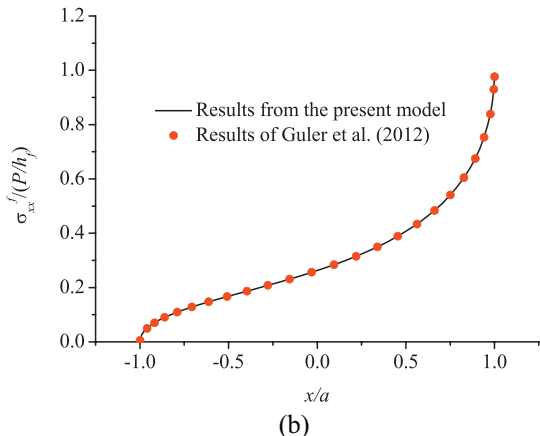
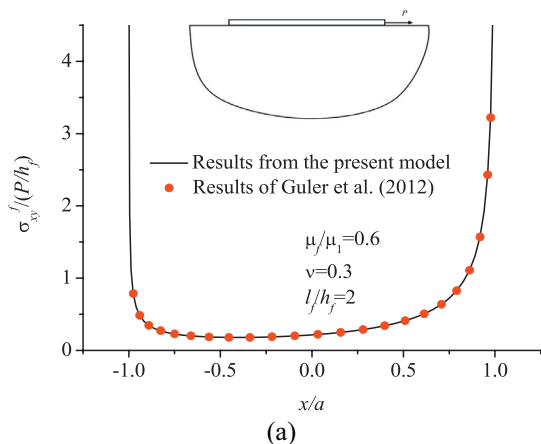


Fig. 4. Comparison of the nondimensional interfacial shear stress $\sigma_{xy}^f(x,0)/(P/h_f)$ and the normal stress in the thin-film $\sigma_{xx}^f(x,0)/(P/h_f)$ for the model of a film in adhesive contact with a homogeneous half plane and the present one with a relatively thick substrate under a loading at a single film end, where $\mu_f/\mu_1=0.6$ and $l_f/h_f=2$.

$$\frac{\partial v(x,0)}{\partial x} = -\frac{\kappa-1}{4\mu_1}\sigma_{xy}(x,0) - \frac{\kappa+1}{4\pi\mu_1}\int_{-a}^a \frac{\sigma_{yy}(r,0)}{r-x}dr + \frac{1}{\pi}\int_{-a}^a [K_{21}(x,r)\sigma_{xy}(r,0) + K_{22}(x,r)\sigma_{yy}(r,0)]dr. \quad (6)$$

where $\sigma_{xy}(x,0)$ is the interfacial shear stress and $\sigma_{yy}(x,0)$ is the normal one between the graded substrate and the bonded film, and $K_{ij}(x,r)$ are bounded functions given in the Appendix.

The film thickness h_f is assumed to be sufficiently small so that membrane assumption holds in the present model. The film is as-

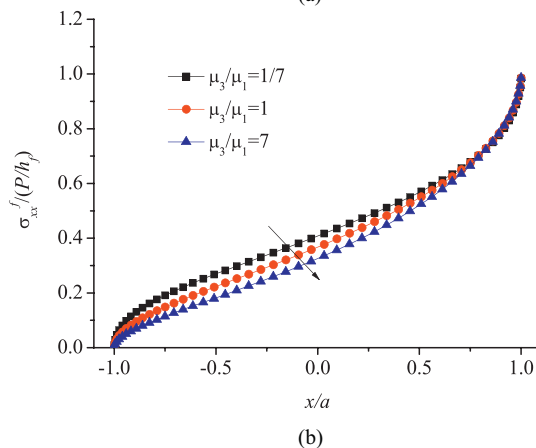
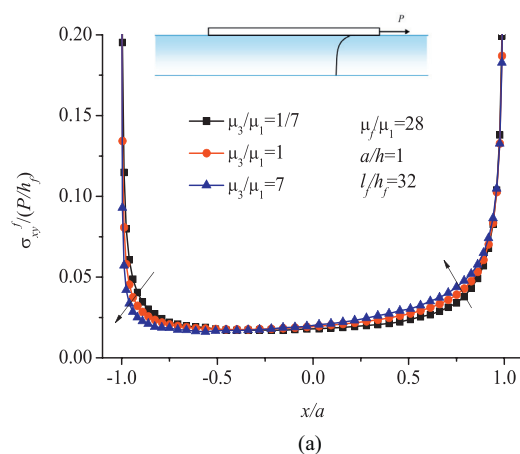


Fig. 5. The distribution of the nondimensional interfacial shear stress $\sigma_{xy}^f(x,0)/(P/h_f)$ and the normal stress in the thin-film $\sigma_{xx}^f(x,0)/(P/h_f)$ for the model of an elastic film bonded to a finite-thickness graded substrate with determined $\mu_f/\mu_1=28$, $a/h=1$ and $l_f/h_f=32$, but with different ratios μ_3/μ_1 .

sumed perfectly bonded to the finite-thickness graded substrate without any initial stress, and only the interfacial shear stress is generated between the film and the substrate when loads are exerted, i.e.,

$$\sigma_{xy}(x,0) = \sigma_{xy}^f(x,0) = \begin{cases} 0, & x < -a, x > a, \\ -f(x), & -a < x < a, \end{cases} \quad (7)$$

$$\sigma_{yy}(x,0) = \sigma_{yy}^f(x,0) = 0, \quad (8)$$

where the superscript 'f' refers to the film.

Due to a small value of the film thickness, the normal stress in the film is assumed to be uniform across the thickness. Based on the equilibrium diagram in Fig 2, one can readily find,

$$Q - \int_{-a}^x \sigma_{xy}^f(r,0)dr = \sigma_{xx}^f(x,0)h_f, \quad (9)$$

and

$$\int_{-a}^a \sigma_{xy}^f(r,0)dr = -\int_{-a}^a f(r)dr = Q - P, \quad (10)$$

where P and Q are loads per unit length exerted at the right and left edges of the film, respectively.

Therefore, the normal stress in the film $\sigma_{xx}^f(x,0)$ can be written as,

$$\sigma_{xx}^f(x,0) = \frac{Q}{h_f} + \frac{1}{h_f}\int_{-a}^x f(r)dr, \quad (11)$$

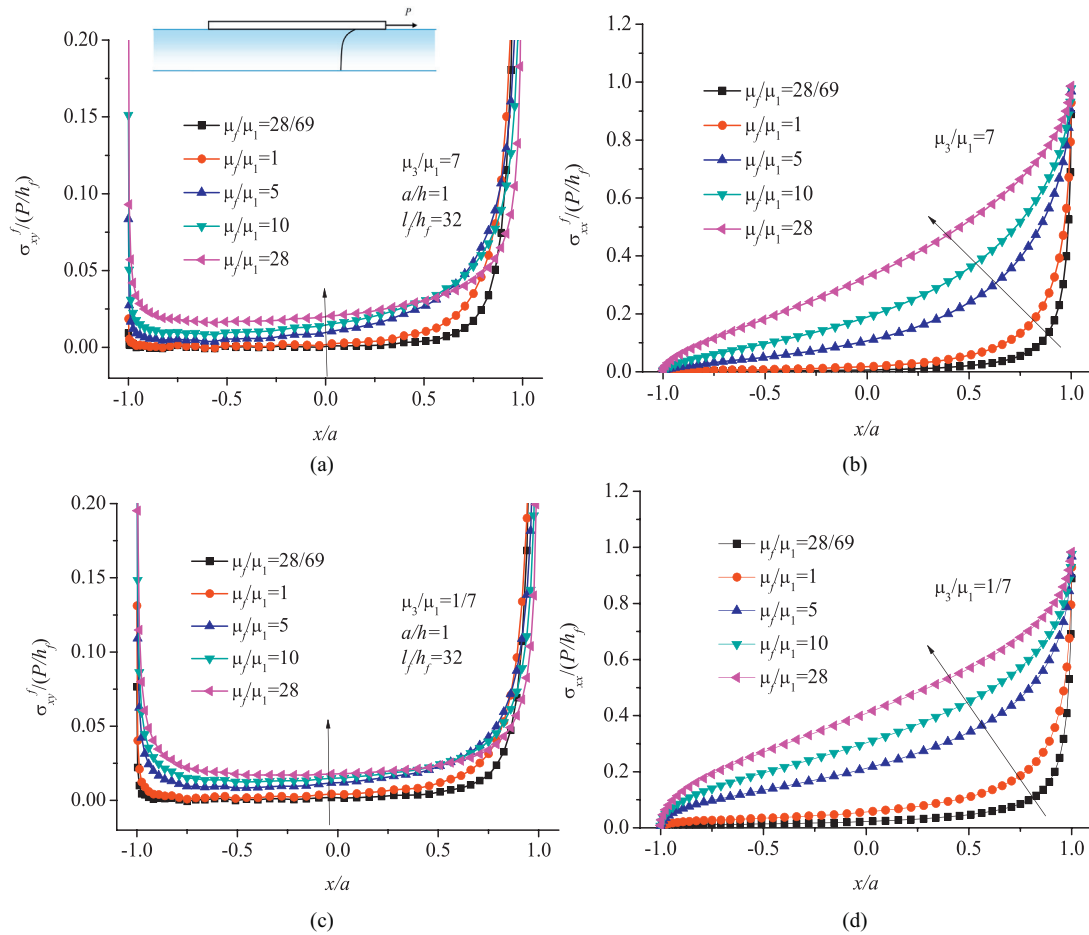


Fig. 6. The distribution of the nondimensional interfacial shear stress $\sigma_{xy}^f(x, 0)/(P/h_f)$ and the normal stress in the thin-film $\sigma_{xx}^f(x, 0)/(P/h_f)$ for the model of an elastic film bonded to a finite-thickness graded substrate with determined $a/h=1$ and $l_f/h_f=32$, but with different ratios μ_j/μ_1 . (a) and (b) for $\mu_3/\mu_1=7$; (c) and (d) for $\mu_3/\mu_1=1/7$.

and the normal strain in the film induced by the interface stress is

$$\varepsilon_{xx}^f(x, 0) = \frac{\partial u^f}{\partial x} = \frac{1 + \kappa_f}{8\mu_f} \sigma_{xx}^f(x, 0), \tag{12}$$

i.e.,

$$\varepsilon_{xx}^f(x, 0) = \frac{1 + \kappa_f}{8\mu_f} \left(\frac{Q}{h_f} + \frac{1}{h_f} \int_{-a}^x f(r) dr \right), \tag{13}$$

where $\kappa_f=3-4\nu_f$ for the plane strain problem and $\kappa_f=(3-\nu_f)/(1+\nu_f)$ for the plane stress one.

From Eq. (5), the strain at the surface of the graded substrate may be written as,

$$\varepsilon_{xx}(x, 0) = \frac{\partial u(x, 0)}{\partial x} = -\frac{\kappa + 1}{4\pi\mu_1} \int_{-a}^a \frac{\sigma_{xy}(r, 0)}{r-x} dr + \frac{1}{\pi} \int_{-a}^a K_{11}(x, r) \sigma_{xy}(r, 0) dr. \tag{14}$$

Besides the loads exerted at the ends of the film, the mismatch strain between the film and the graded substrate $\varepsilon_0(x)$ can also be taken into consideration, for example, a constant strain $\varepsilon_0=[(1+\nu)\alpha-(1+\nu_f)\alpha_f]\Delta T$ might be caused by a uniform temperature change ΔT at the same time, where α and α_f are the thermal expansion coefficients of the graded substrate and the film, respectively.

Thus, the compatibility condition at the interface can be given as,

$$\varepsilon_{xx}(x, 0) - \varepsilon_{xx}^f(x, 0) = \varepsilon_0(x). \tag{15}$$

Combining Eqs. (13)–(15) yields the governing equation of the present model, i.e.,

$$\frac{1}{\pi} \int_{-a}^a \left[\frac{1}{r-x} - \frac{4\mu_1}{\kappa+1} K_{11}(x, r) \right] f(r) dr - \frac{\chi}{2h_f} \int_{-a}^x f(r) dr = \frac{\chi}{2h_f} Q + \frac{4\mu_1}{\kappa+1} \varepsilon_0(x), \tag{16}$$

where $\chi = \frac{1+\kappa_f}{1+\kappa} \frac{\mu_1}{\mu_f}$ is a parameter determining the compliancy between the film and the surface layer of the graded substrate.

4. Solutions to the integral equation

As shown in Fig. 3(a) and (b), basic mechanical loadings of the film/substrate system consist of single loading on the film and mismatch strain loading at the interface. Based on the fundamental solutions under these basic loadings, the problems involving more complicated loadings could be solved with the help of superposition method. In the following, the fundamental solutions are studied for the interfacial mechanics in the film/substrate systems under these basic mechanical loadings.

4.1. Loading at a single end of the film

When $Q=0$ and $\varepsilon_0(x)=0$, the model shown in Fig. 1 will reduce to a special one that is, a film with loading at a single end. By introducing the following normalized definition

$$x = as, \quad r = at, \tag{17}$$

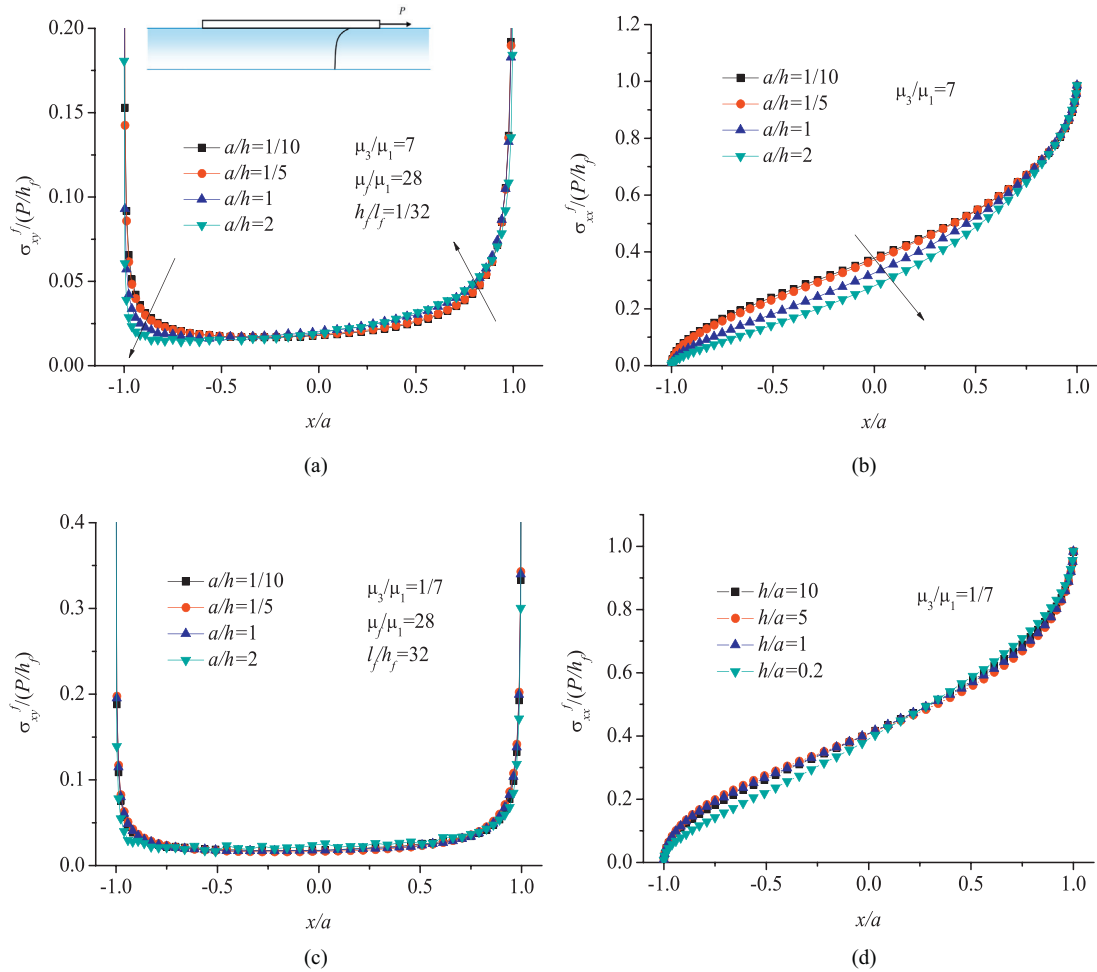


Fig. 7. The distribution of the nondimensional interfacial shear stress $\sigma_{xy}^f(x, 0)/(P/h_f)$ and the normal stress in the thin-film $\sigma_{xx}^f(x, 0)/(P/h_f)$ for the model of an elastic film bonded to a finite-thickness graded substrate with determined $\mu_3/\mu_1=28$ and $l_f/h_f=32$, but with different ratio a/h . (a) and (b) for $\mu_3/\mu_1=7$; (c) and (d) for $\mu_3/\mu_1=1/7$.

the governing equation in Eq. (16) and the equilibrium equation in Eq. (10) becomes,

$$\frac{1}{\pi} \int_{-1}^1 \left[\frac{1}{t-s} - \frac{4\mu_1 a}{\kappa+1} K_{11}(s, t) \right] f(t) dt - \frac{a\chi}{2h_f} \int_{-1}^s f(t) dt = 0, \quad (18)$$

$$\int_{-1}^1 f(t) dt = -\frac{P}{a}. \quad (19)$$

Due to the Cauchy-type singular kernel in the governing equation, the solution to Eqs. (18) and (19) could be expressed as (Gladwell, 1980; Guler, 2008),

$$f(s) = \frac{1}{\sqrt{1-s^2}} \sum_{n=0}^{\infty} A_n T_n(s), \quad (20)$$

where $T_n(\cdot)$ is the Chebyshev polynomial of the first kind of order n , A_n denotes unknown constant to be determined.

Taking into consideration the properties of Chebyshev polynomials in the Appendix, Eq. (18) can be reduced to

$$\sum_{n=1}^{\infty} A_n [U_{n-1}(s) + Q_n(s)] = F(s), \quad |s| \leq 1, \quad (21)$$

where,

$$Q_n(s) = -\frac{1}{\pi} \int_{-1}^1 \frac{4\mu_1 a}{\kappa+1} K_{11}(s, t) \frac{T_n(t)}{\sqrt{1-t^2}} dt + \frac{\chi a}{2h_f} \frac{1}{n} U_{n-1}(s) \sqrt{1-s^2}, \quad (22)$$

$$F(s) = A_0 \left\{ \frac{\chi a}{2h_f} [\pi - \cos^{-1}(as)] + \frac{1}{\pi} \int_{-1}^1 \frac{4\mu_1 a}{1+\kappa} \frac{K_{11}(s, t)}{\sqrt{1-t^2}} ds \right\}. \quad (23)$$

The value of A_0 can be readily obtained from Eq. (19) as

$$A_0 = -\frac{P}{\pi a}. \quad (24)$$

Thus, the governing integral Eq. (18) can be reduced to a system of algebraic Eq. (21) in terms of the unknown constants A_n . Truncating the infinite series at $n=N$ and selecting suitable collocation points as roots of the following Chebyshev polynomials (Erdogan et al., 1973),

$$T_N(s_i) = 0, \quad i = 1, \dots, N, \quad (25)$$

the system of algebraic equations can be well solved with N unknown constants A_n ($n=1, 2, \dots, N$).

The interfacial shear stress $\sigma_{xy}^f(x, 0)$ can be approximately given as,

$$\sigma_{xy}^f(x, 0) = -f(x) = -\frac{\sum_{n=0}^N A_n T_n(x/a)}{\sqrt{1-(x/a)^2}}. \quad (26)$$

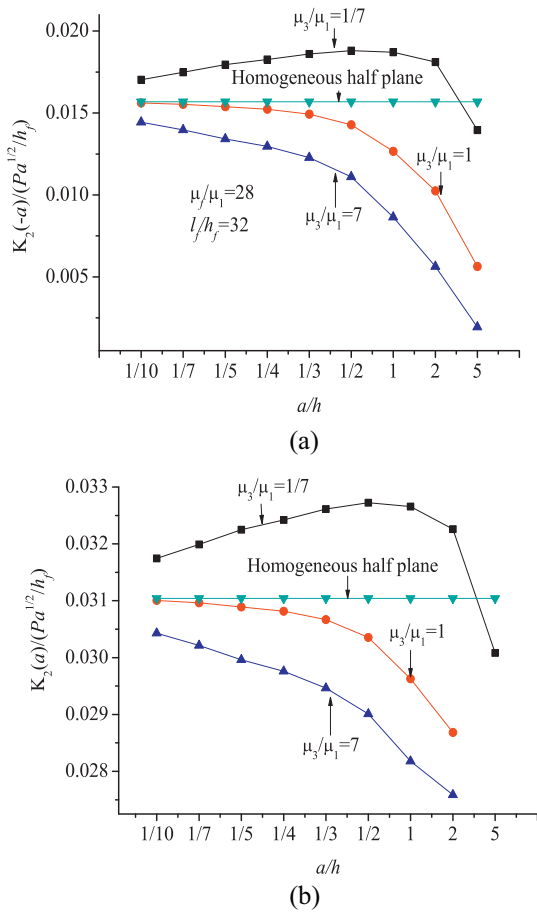


Fig. 8. Variation of the stress intensity factors $K_2(-a)/(P\sqrt{a}/h_f)$ and $K_2(a)/(P\sqrt{a}/h_f)$ near film ends versus the ratio of half of the film length to the substrate thickness a/h for different ratios μ_3/μ_1 , where $\mu_f/\mu_1=28$, $l_f/h_f=32$.

Then, the normal stress in the film becomes,

$$\sigma_{xx}^f(x, 0) = \frac{1}{h_f} \left\{ -aA_0[\pi - \cos^{-1}(x/a)] + a \sum_{n=1}^N \frac{A_n}{n} U_{n-1}\left(\frac{x}{a}\right) \sqrt{1 - \left(\frac{x}{a}\right)^2} \right\}. \quad (27)$$

The shear stress singularities at the left and right end of the thin film can be expressed as

$$\frac{K_2(-a)}{P\sqrt{a}/h_f} = - \sum_{n=0}^N A_n T_n(-1), \quad (28)$$

$$\frac{K_2(a)}{P\sqrt{a}/h_f} = - \sum_{n=0}^N A_n T_n(1). \quad (29)$$

4.2. A mismatch loading in the film/substrate system

When $P=Q=0$ is chosen in Fig. 1, the applied loading in the film/substrate system is reduced to the case of a mismatch strain at the interface as shown in Fig. 3(b). For better understanding and simplicity, $\varepsilon_0(x)$ is usually assumed to be a constant, i.e., $\varepsilon_0(x)=\varepsilon_0$.

The solution to the governing integral Eq. (16) can also be expressed as those in Eq. (20) for this case. Considering the orthogonality of the Chebyshev polynomials, one can readily obtain,

$$A_0 = 0, \quad (30)$$

and

$$\sum_{n=1}^{\infty} A_n [U_{n-1}(s) + Q_n(s)] = \frac{4\mu_1}{\kappa + 1} \varepsilon_0, \quad |s| \leq 1, \quad (31)$$

where

$$Q_n(s) = -\frac{1}{\pi} \int_{-1}^1 \frac{4\mu_1 a}{\kappa + 1} K_{11}(s, t) \frac{T_n(t)}{\sqrt{1-t^2}} dt + \frac{\chi a}{2h_f} \frac{1}{n} U_{n-1}(s) \sqrt{1-s^2}. \quad (32)$$

Based on the solutions to Eq. (31) and taking into consideration the symmetry of this problem, we can find the shear stress singularities at the both ends of the thin film, i.e.,

$$\frac{K_2(-a)}{4\mu_1 \varepsilon_0 \sqrt{a}/(\kappa + 1)} = \frac{K_2(a)}{4\mu_1 \varepsilon_0 \sqrt{a}/(\kappa + 1)} = - \sum_{n=0}^N A_n T_n(-1), \quad (33)$$

For the bonded problem between a thin-film and a finite graded substrate subjected to a mismatch loading, detailed analysis can be found in our recent work (Chen et al., 2016b).

After obtaining the fundamental solutions under these basic loading cases, the problems involving more complicated loadings can be determined by using the superposition method.

5. Results and discussion

In the following section, interfacial properties of a thin film bonded to a finite-thickness graded substrate are explored. Throughout the analysis, a plane strain condition is adopted, and the Poisson's ratios of the film and the substrate are the same, $\nu=\nu_f=0.3$. The symmetrical loading case has been discussed in detail for the graded substrate in our previous work (a mismatch loading case in Chen et al. (2016b)). Therefore, the interfacial properties of the film/substrate system under unsymmetrical loadings are mainly focused in the following analysis.

Note that the analyses in the present paper and those in Chidlow et al. (2011, 2012) are totally different. Chidlow et al. (2011, 2012) have proposed a Fourier series based solution method to analyze the sub-surface stresses and local deflection of a graded medium loaded by a pre-determined pressure and a rigid punch (a contact model of a single deformable solid). The stresses in Chidlow et al. (2011, 2012)'s model vanish at the deformable solid's edge because of Saint-Venant's Principle. However, for the bonded problem in the present paper, the elastic film is of a finite length, and the effect of the film edges cannot be neglected. What's more, the stresses at the film edges provide the most important information, because that the interface near the film edges are the most vulnerable place for the film/substrate system. Difference between the present model and the one in Chidlow et al. (2011, 2012) includes also the final results. In Chidlow et al. (2011, 2012)'s result, the sub-surface stress field in the solid is calculated loaded by a pre-determined pressure and a rigid punch. However, the interfacial shear stress, the normal stress in the film as well as the stress singularities near the film edges induced by different loadings are mainly discussed in the present paper to evaluate the interface behaviors that are closely related to failure and destruction of the film/graded substrate systems.

When $\gamma=0$ and $h/a \rightarrow \infty$ in the present model, the finite-thickness graded substrate will reduced to a special one, i.e., an homogeneous half plane. The distribution of the nondimensional interfacial shear stress $\sigma_{xy}^f(x, 0)/(P/h_f)$ and the normal stress in the thin-film $\sigma_{xx}^f(x, 0)/(P/h_f)$ under a loading at a single film end for the homogeneous half plane is shown in Fig. 4(a) and (b), in which we take $\mu_f/\mu_1=0.6$ and $l_f/h_f=2$. One can readily find that non-symmetric stresses are induced due to the non-symmetric loading. The interfacial shear stress increases dramatically toward each

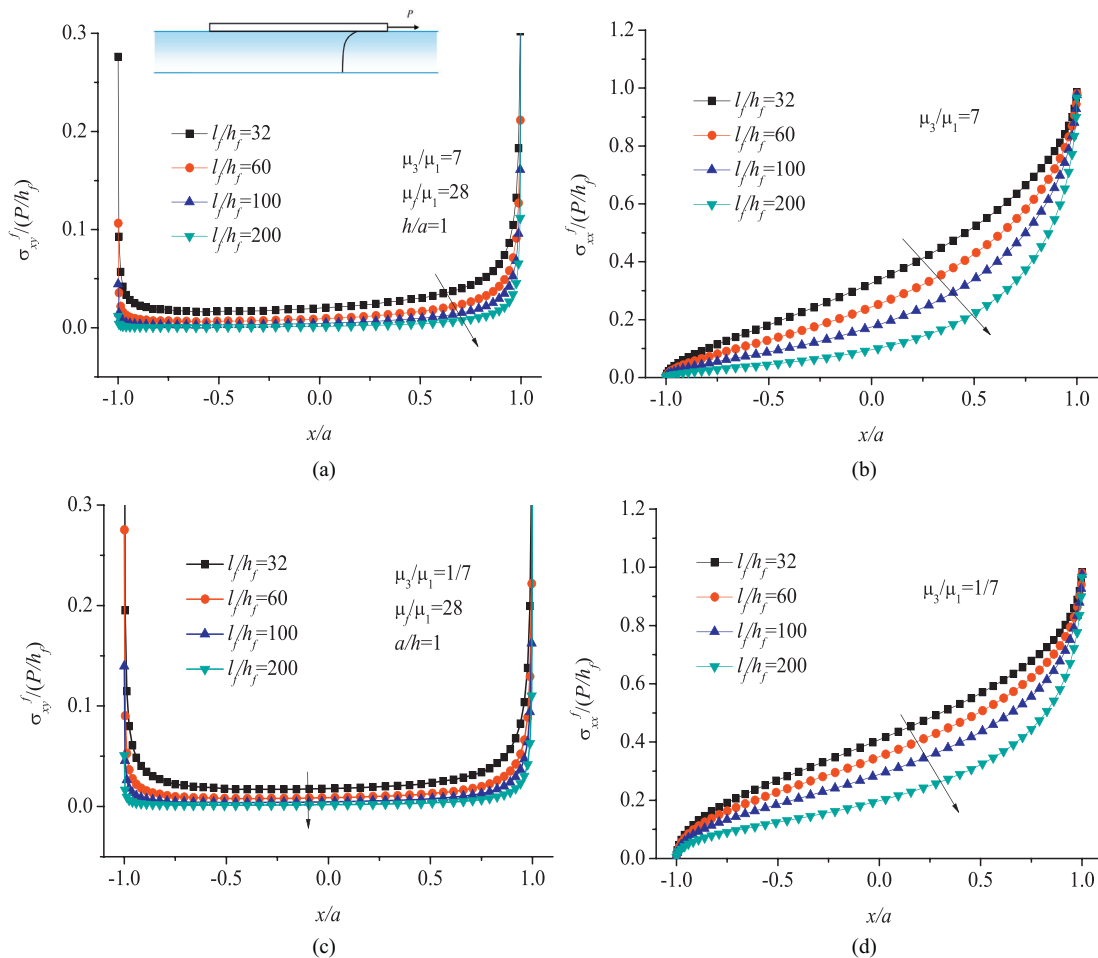


Fig. 9. The distribution of the nondimensional interfacial shear stress $\sigma_{xy}^f(x, 0)/(P/h_f)$ and the normal stress in the thin-film $\sigma_{xx}^f(x, 0)/(P/h_f)$ for the model of an elastic film bonded to a finite-thickness graded substrate with determined $\mu_f/\mu_1=28$ and $a/h=1$, but with different ratios l_f/h_f . (a) and (b) for $\mu_3/\mu_1=7$; (c) and (d) for $\mu_3/\mu_1=1/7$.

Table 1

Variation of the Mode II stress intensity factors near both ends, $K_2(-a)/(P\sqrt{a}/h_f)$ and $K_2(a)/(P\sqrt{a}/h_f)$ for selected ratio of shear modulus μ_3/μ_1 in cases of determined parameters $\mu_f/\mu_1=28$, $a/h=1$ and $l_f/h_f=32$.

	$\mu_3/\mu_1=1/7$	$\mu_3/\mu_1=1$	$\mu_3/\mu_1=7$
$K_2(-a)/(P\sqrt{a}/h_f)$	0.0187	0.0127	0.0086
$K_2(a)/(P\sqrt{a}/h_f)$	0.0327	0.0296	0.0282

end and is obvious singular near both ends of the film. The normal stress in the film equals the value of the dimensionless applied load P/h_f at the loaded end, while remaining zero at the free end. The results obtained from the present model agree well with those reported by Guler et al. (2012). Thus, the proposed model can be seen as the extending of the existing bonded problems of the film/elastic homogeneous substrate system.

When it comes to graded substrates, comprehensive analyses of the effect of different parameters are given in Figs. 5–11. Fig. 5(a) and (b) shows the effect of the ratio of shear modulus μ_3/μ_1 on the distributions of interfacial shear stress and the normal stress in the film, respectively, in which $\mu_f/\mu_1=28$, $a/h=1$ and $l_f/h_f=32$. From Fig. 5(a), the interfacial shear stress at both the free and loaded ends of the film varies when different μ_3/μ_1 is chosen. Variation of the corresponding Mode II stress intensity factors near both ends, $K_2(-a)/(P\sqrt{a}/h_f)$ and $K_2(a)/(P\sqrt{a}/h_f)$ is given in Table 1. Obviously, the stress intensity factors at the free end are

much less than those at the loaded one, and the values at both ends decrease with an increasing μ_3/μ_1 . The normal stress in the film is found to decrease with an increasing μ_3/μ_1 in the bonded area. All results suggest that, for a thin-film bonded to a finite-thickness graded substrate under a single film loading, a substrate with an increasing modulus in the thickness is beneficial to a more reliable interface and a more durable film.

The distribution of the nondimensional interfacial shear stress $\sigma_{xy}^f(x, 0)/(P/h_f)$ and the nondimensional normal stress $\sigma_{xx}^f(x, 0)/(P/h_f)$ in the film as a function of the ratio μ_f/μ_1 is shown in Fig. 6. A fixed value $\mu_3/\mu_1=7$ is used in Fig. 6(a) and (b), while $\mu_3/\mu_1=1/7$ is adopted in Fig. 6(c) and (d). One can readily find that both the interfacial shear stress and the normal stress in the film increase with μ_f/μ_1 no matter what value μ_3/μ_1 is chosen. The corresponding Mode II stress intensity factor is given in Table 2, specifically, the factors at the free end increase while the ones at the loaded end decrease significantly when μ_f/μ_1 increases. However, the stress intensity factors at both ends have been found to increase with an increasing μ_f/μ_1 under a mismatch strain loading (Chen et al., 2016b), which shows a totally different variation trend under the present single film end loading. This phenomenon has been reported by Lanzoni (2011), in which an elastic film bonded to a homogeneous half plane is discussed.

The ratio effect of contact region to the thickness of the substrate a/h on the interfacial stress and the normal stress in the film is given in Fig. 7. Fig. 7(a) and (b) correspond to the cases of a substrate with an increasing modulus along the thickness $\mu_3/\mu_1=7$,

Table 2

The stress intensity factors $K_2(-a)/(P\sqrt{a}/h_f)$ and $K_2(a)/(P\sqrt{a}/h_f)$ near both ends versus different ratios μ_f/μ_1 in cases with fixed parameters $a/h=1$, $l_f/h_f=32$ and μ_3/μ_1 .

μ_f/μ_1	$\mu_3/\mu_1=1/7$		$\mu_3/\mu_1=7$	
	$\frac{K_2(-a)}{(P\sqrt{a}/h_f)}$	$\frac{K_2(a)}{(P\sqrt{a}/h_f)}$	$\frac{K_2(-a)}{(P\sqrt{a}/h_f)}$	$\frac{K_2(a)}{(P\sqrt{a}/h_f)}$
28/69	0.0003	0.2221	0.0003	0.2220
1	0.0004	0.1417	0.0006	0.1416
5	0.0106	0.0642	0.0026	0.0635
10	0.0143	0.0470	0.0047	0.0451
28	0.0187	0.0327	0.0086	0.0282

Table 3

Variation of the Mode II stress intensity factors near both ends, $K_2(-a)/(P\sqrt{a}/h_f)$ and $K_2(a)/(P\sqrt{a}/h_f)$ for selected ratio of the film thickness to its thickness l_f/h_f in cases of determined parameters $\mu_f/\mu_1=28$, $a/h=1$ and μ_3/μ_1 .

l_f/h_f	$\mu_3/\mu_1=1/7$		$\mu_3/\mu_1=7$	
	$\frac{K_2(-a)}{(P\sqrt{a}/h_f)}$	$\frac{K_2(a)}{(P\sqrt{a}/h_f)}$	$\frac{K_2(-a)}{(P\sqrt{a}/h_f)}$	$\frac{K_2(a)}{(P\sqrt{a}/h_f)}$
32	0.0187	0.0327	0.0086	0.0282
60	0.0087	0.0214	0.0033	0.0199
100	0.0044	0.0158	0.0014	0.0152
200	0.0016	0.0108	0.0004	0.0107

while Fig. 7(c) and (d) correspond to those with a decreasing stiffness $\mu_3/\mu_1=1/7$. The a/h shows a more regular effect on the interfacial stress and the normal stress in the film for the form cases, in which both stresses vary monotonically with an increasing a/h . However, nonmonotonical variation of the interfacial shear stress and the normal stress in the film can be found for the latter cases in Fig. 7(c) and (d). Variation of the corresponding Mode II stress intensity factors at both the film edges versus the nondimensional contact region a/h for different μ_3/μ_1 is shown in Fig. 8(a) and (b), where the result of a homogeneous half plane case is also given for comparison. It is easily found that both $K_2(-a)/(P\sqrt{a}/h_f)$ and $K_2(a)/(P\sqrt{a}/h_f)$ decrease monotonically with a/h for the cases of $\mu_3/\mu_1 \geq 1$, while increase first then decrease for the case of $\mu_3/\mu_1 < 1$. Therefore, the ratio effect of contact region to the thickness of the substrate on the interfacial properties can not be neglected. The results of a finite substrate cannot be predicted by an infinite model. However, if $a/h \rightarrow 0$, the ratio effect weakens in all cases and the intensity factors at both edges tend to the case of a homogeneous half plane.

Fig. 9 displays the distributions of the interfacial shear stress and the normal stress in the film affected by the parameter of the ratio of the film thickness to its thickness l_f/h_f . A fixed value $\mu_3/\mu_1=7$ is chosen in Fig. 9(a) and (b), while $\mu_3/\mu_1=1/7$ is adopted in Fig. 9(c) and (d). Similar changes of the interfacial shear stress and the normal stress in the film can be easily found for the cases of and those of $\mu_3/\mu_1=1/7$. In both cases, the interfacial shear stress as well as the normal stress in the film decrease with an increasing l_f/h_f . The corresponding Mode II stress intensity factors are listed in Table 3, from which one can readily notice that both $K_2(-a)/(P\sqrt{a}/h_f)$ and $K_2(a)/(P\sqrt{a}/h_f)$ decrease with an increasing l_f/h_f . Therefore, we can infer that for a fixed film length, the thinner the film, the stronger the interface strength is; while for cases of a fixed film thickness, the longer the film is, the more reliable interface behavior it will lead.

Furthermore, two opposite loadings applied at both ends of the film will lead to the film/substrate system under a symmetric loading as shown in Fig. 10, which can be tackled through a superposition of single end film loading cases. Note that the bonded problem involving more complicated loadings can also be well determined

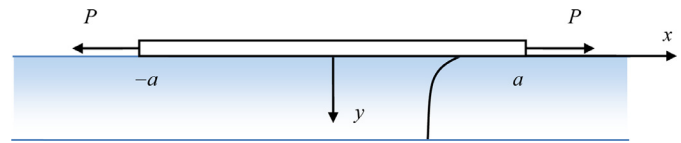


Fig. 10. The bonded model between an elastic film and a graded substrate under two opposite loadings at the ends of the film.

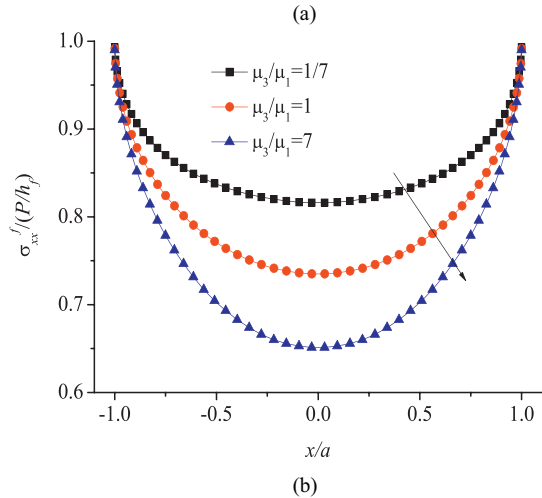
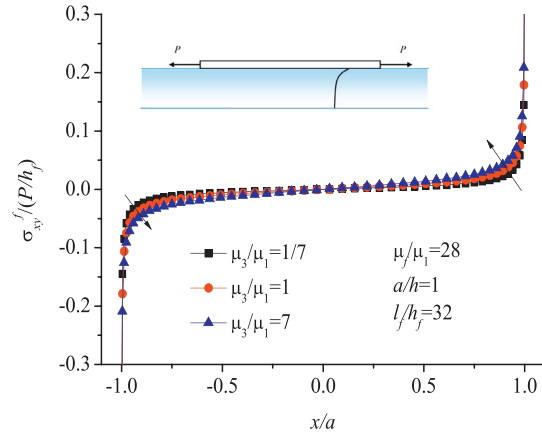


Fig. 11. The distribution of the nondimensional interfacial shear stress $\sigma_{xy}^f(x, 0)/(P/h_f)$ and the normal stress in the thin-film $\sigma_{xx}^f(x, 0)/(P/h_f)$ for the model of an elastic film bonded to a finite-thickness graded substrate under two opposite loadings at the film ends with different ratios μ_3/μ_1 , and fixed $\mu_f/\mu_1=28$, $a/h=1$ and $l_f/h_f=32$.

Table 4

The stress intensity factors $K_2(-a)/(P\sqrt{a}/h_f)$ and $K_2(a)/(P\sqrt{a}/h_f)$ near both ends versus different ratios μ_3/μ_1 for the cases of two opposite loadings at the ends of a film, and fixed parameters $\mu_f/\mu_1=28$, $a/h=1$, $l_f/h_f=32$.

	$\mu_3/\mu_1=1/7$	$\mu_3/\mu_1=1$	$\mu_3/\mu_1=7$
$K_2(-a)/(P\sqrt{a}/h_f)$	0.0140	0.0170	0.0195
$K_2(a)/(P\sqrt{a}/h_f)$	0.0140	0.0170	0.0195

with the help of superposition method. Distributions of the nondimensional interfacial shear stress $\sigma_{xy}^f(x, 0)/(P/h_f)$ and the normal stress in the thin-film $\sigma_{xx}^f(x, 0)/(P/h_f)$ for the symmetric loading case as a function of the ratio μ_3/μ_1 are shown in Fig. 11. The variations of $K_2(-a)/(P\sqrt{a}/h_f)$ and $K_2(a)/(P\sqrt{a}/h_f)$ are presented in Table 4. Obviously, the stress intensity factors at both ends are equal, and the values increase with an increasing μ_3/μ_1 . It means a substrate with a decreasing stiffness will lead to more reliable

interface, which agrees very well with the findings in Chen et al., (2016b), but it presents a totally different variation trend from the findings for a single film end loading case given above. Similar to the ratio effect of μ_f/μ_1 , the effect of the shear modulus ratio μ_3/μ_1 are found to be dependent of the applied loadings.

6. Conclusions

The non-slipping contact model of an elastic film on a finite-thickness graded substrate under different loading conditions is investigated in the present paper. With the help of Fourier transform and numerical calculation, the distribution of the interfacial shear stress, the normal stress in the film as well as the corresponding Mode II intensity factors are analyzed by solving the governing singular integral equation. It is found that (i) The bonded problem of an elastic film on a graded substrate under both the non-symmetric loading condition and the symmetric one can be effectively modeled; (ii) The interface behavior of the film/substrate system can be modified by tuning the film stiffness, the stiffness variation of the graded substrate, as well as the geometric parameters of the film and substrate; (iii) Compared with cases under both a single film end loading and a symmetric one, the effect of the modulus ratio effect of the film to the upper surface of the substrate μ_f/μ_1 and the stiffness variation of the graded substrate μ_3/μ_1 is observed to be dependent of the applied loading. The result should be very useful for the design of film-substrate systems in potential and practical applications.

Acknowledgement

The authors gratefully acknowledge the support of NSFC (Nos. 11402292, 11404393 and 51579239), Natural Science Foundation of Jiangsu Province (No. BK20140179), the Fundamental Research Funds for the Central Universities (No. 2014QNA61).

Appendix

$K_{ij}(x, r)$ appearing in Eqs. (5) and (6) are expressed as follows,

$$K_{11}(x, r) = \int_0^{+\infty} \left[\alpha \phi_{11}(\alpha) + \frac{\kappa + 1}{4\mu_1} \right] \sin[\alpha(r - x)] d\alpha. \quad (A1a)$$

$$K_{12}(x, r) = - \int_0^{+\infty} \left[\alpha \phi_{12}(\alpha) + \frac{\kappa - 1}{4\mu_1} \right] \cos[\alpha(r - x)] d\alpha, \quad (A1b)$$

$$K_{21}(x, r) = \int_0^{+\infty} \left[\alpha \phi_{21}(\alpha) + \frac{\kappa - 1}{4\mu_1} \right] \cos[\alpha(r - x)] d\alpha, \quad (A1c)$$

$$K_{22}(x, r) = \int_0^{+\infty} \left[\alpha \phi_{22}(\alpha) + \frac{\kappa + 1}{4\mu_1} \right] \sin[\alpha(r - x)] d\alpha, \quad (A1d)$$

where $\phi_{jk}(\alpha)$ are the elements of matrix $\Phi(\alpha)$.

The matrix $\Phi(\alpha)$ can be given as,

$$\Phi(\alpha) = \begin{bmatrix} G_{13} & G_{14} \\ G_{23} & G_{24} \end{bmatrix} \cdot \begin{bmatrix} G_{33} & G_{34} \\ G_{43} & G_{44} \end{bmatrix}^{-1}, \quad (A2)$$

where G_{ij} ($i, j = 1, \dots, 4$) is elements of the matrix $G(\alpha)$, and

$$G(\alpha) = T(\alpha, 0)T^{-1}(\alpha, h). \quad (A3)$$

The elements in the matrix $T(\alpha, y)$ are as follows,

$$T_{1j}(\alpha, y) = e^{n_j y}, \quad (A4a)$$

$$T_{2j}(\alpha, y) = -m_j e^{n_j y}, \quad (A4b)$$

$$T_{3i}(\alpha, y) = \mu_2 [n_j - sm_j] e^{n_j y}. \quad (A4c)$$

$$T_{4i}(\alpha, y) = \frac{\mu_2 [m_j n_j (\kappa + 1) + (3 - \kappa)s]}{(1 - \kappa)} e^{n_j y}, \quad (j = 1, \dots, 4) \quad (A4d)$$

n_j, m_j ($j = 1, \dots, 4$) appearing in Eq. (A4) are as follows,

$$n_j(\alpha) = -\frac{\gamma}{2} + \sqrt{\frac{\gamma^2}{4} + \alpha^2 - i(-1)^j \gamma \alpha \left(\frac{3 - \kappa}{1 + \kappa} \right)^{1/2}},$$

$$\text{Re}(n_j) > 0, \quad j = 1, 2, \quad (A5)$$

$$n_j(\alpha) = -\frac{\gamma}{2} - \sqrt{\frac{\gamma^2}{4} + \alpha^2 + i(-1)^j \gamma \alpha \left(\frac{3 - \kappa}{1 + \kappa} \right)^{1/2}},$$

$$\text{Re}(n_j) < 0, \quad j = 3, 4, \quad (A6)$$

$$m_j(\alpha) = \frac{(\kappa - 1)(n_j^2 + \gamma n_j) - \alpha^2(\kappa + 1)}{\alpha [2n_j + \gamma(\kappa - 1)]}, \quad (j = 1, \dots, 4), \quad (A7)$$

The properties of Chebyshev polynomials used in Eq. (21) are given as follows:

$$\frac{1}{\pi} \int_{-1}^1 \frac{T_n(t)}{(t-s)\sqrt{1-t^2}} dt = \begin{cases} 0, & n = 0 \\ U_{n-1}(s), & n > 0 \end{cases} \quad |s| \leq 1 \quad (A8)$$

$$\int_{-1}^s \frac{T_n(t)}{\sqrt{1-t^2}} dt = -\frac{1}{n} U_{n-1}(s) \sqrt{1-s^2} \quad |s| \leq 1, \quad (A9)$$

$$\frac{1}{\pi} \int_{-1}^1 \frac{T_n(t)T_m(t)}{\sqrt{1-t^2}} ds = \begin{cases} 0, & m \neq n \\ 1, & m = n = 0 \\ 1/2, & m = n \geq 1 \end{cases} \quad (A10)$$

References

- Akisanya, A.R., Fleck, N.A., 1994. The edge cracking and decohesion of thin films. *Int. J. Solids Struct.* 31, 3175–3199.
- Alaca, B.E., Saif, M.T.A., Sehitoglu, H., 2002. On the interface debond at the edge of a thin film on a thick substrate. *Acta Mater.* 50, 1197–1209.
- Arutiunian, N.K., 1968. Contact problem for a half-plane with elastic reinforcement. *Pmm-J. Appl. Math. Mech.* 32, 652–665.
- Banerjee, S., Marchetti, M.C., 2012. Contractile stresses in cohesive cell layers on finite-thickness substrates. *Phys. Rev. Lett.* 109, 108101.
- Booker, J.R., Balaam, N.P., Davis, E.H., 1985. The behavior of an elastic non-homogeneous half-space.1. line and point loads. *Int. J. Numer. Anal. Methods Geomech.* 9, 353–367.
- Chen, P., Chen, S., 2013a. Partial slip contact between a rigid punch with an arbitrary tip-shape and an elastic graded solid with a finite thickness. *Mech. Mater.* 59, 24–35.
- Chen, P., Chen, S., 2013b. Thermo-mechanical contact behavior of a finite graded layer under a sliding punch with heat generation. *Int. J. Solids Struct.* 50, 1108–1119.
- Chen, P., Chen, S., Peng, J., 2015. Sliding contact between a cylindrical punch and a graded half-plane with an arbitrary gradient direction. *J. Appl. Mech.-Trans. ASME* 82, 041008.
- Chen, P., Chen, S., Peng, J., 2016a. Interface behavior of a thin-film bonded to a graded layer coated elastic half-plane. *Int. J. Mech. Sci.* 115–116, 489–500.
- Chen, P., Chen, S., Yao, Y., 2016b. Nonslipping contact between a mismatch film and a finite-thickness graded substrate. *J. Appl. Mech.-Trans. ASME* 83, 021007.
- Chidlow, S., Teodorescu, M., Vaughan, N., 2011. Predicting the deflection and sub-surface stress field within two-dimensional inhomogeneously elastic bonded layered solids under pressure. *Int. J. Solids Struct.* 48, 3243–3256.
- Chidlow, S., Teodorescu, M., Vaughan, N., 2012. A solution method for the sub-surface stresses and local deflection of a semi-infinite inhomogeneous elastic medium. *Appl. Math. Model.* 36, 3486–3501.
- Choi, H.J., Paulino, G.H., 2008. Thermoelastic contact mechanics for a flat punch sliding over a graded coating/substrate system with frictional heat generation. *J. Mech. Phys. Solids* 56, 1673–1692.
- Choi, H.J., Paulino, G.H., 2010. Interfacial cracking in a graded coating/substrate system loaded by a frictional sliding flat punch. *Proc. R. Soc. A-Math. Phys. Eng. Sci.* 466, 853–880.
- Dag, S., Apatay, T., Gulcer, M.A., Gulcer, M., 2012. A surface crack in a graded coating subjected to sliding frictional contact. *Eng. Fract. Mech.* 80, 72–91.
- Dai, L.C., Huang, Y., Chen, H., Feng, X., Fang, D.N., 2015. Transition among failure modes of the bending system with a stiff film on a soft substrate. *Appl. Phys. Lett.* 106.
- Elloumi, R., Kallel-Kamoun, I., El-Borgi, S., 2010. A fully coupled partial slip contact problem in a graded half-plane. *Mech. Mater.* 42, 417–428.

- Erdogan, F., Gupta, G.D., 1971. The problem of an elastic stiffener bonded to a half plane. *J. Appl. Mech.-Trans. ASME* 38, 937–941.
- Erdogan, F., Gupta, G.D., Cook, T.S., 1973. Numerical solution of singular integral equations. In: Sih, G. (Ed.), *Methods of Analysis and Solutions of Crack Problems*. Springer, Netherlands, pp. 368–425.
- Erdogan, F., Joseph, P.F., 1990a. Mechanical modeling of multilayered films on an elastic substrate-Part I: Analysis. *J. Electron. Packag.* 112, 309–316.
- Erdogan, F., Joseph, P.F., 1990b. Mechanical modeling of multilayered films on an elastic substrate-Part II: results and discussion. *J. Electron. Packag.* 112, 317–326.
- Fang, D., Wang, J., Chen, W., 2013. *Analysis of Piezoelectric Structures and Devices*. Walter de Gruyter.
- Giannakopoulos, A.E., Pallot, P., 2000. Two-dimensional contact analysis of elastic graded materials. *J. Mech. Phys. Solids* 48, 1597–1631.
- Gladwell, G.M.L., 1980. *Contact Problems in the Classical Theory of Elasticity*. Martinus Nijhoff Publishers, The Hague, The Netherlands.
- Guler, M.A., 2008. Mechanical modeling of thin films and cover plates bonded to graded substrates. *J. Appl. Mech.-Trans. ASME* 75, 051105.
- Guler, M.A., Erdogan, F., 2004. Contact mechanics of graded coatings. *Int. J. Solids Struct.* 41, 3865–3889.
- Guler, M.A., Erdogan, F., 2007. The frictional sliding contact problems of rigid parabolic and cylindrical stamps on graded coatings. *Int. J. Mech. Sci.* 49, 161–182.
- Guler, M.A., Gulver, Y.F., Nart, E., 2012. Contact analysis of thin films bonded to graded coatings. *Int. J. Mech. Sci.* 55, 50–64.
- Hu, S.M., 1979. Film-edge-induced stress in substrates. *J. Appl. Phys.* 50, 4661–4666.
- Huang, G., Song, F., Wang, X., 2010. Quantitative modeling of coupled piezo-elastodynamic behavior of piezoelectric actuators bonded to an elastic medium for structural health monitoring: A review. *Sensors* 10, 3681–3702.
- Jin, C., Wang, X., 2011. Analytical modelling of the electromechanical behaviour of surface-bonded piezoelectric actuators including the adhesive layer. *Eng. Fract. Mech.* 78, 2547–2562.
- Jin, F., Guo, X., Gao, H., 2013. Adhesive contact on power-law graded elastic solids: The JKR–DMT transition using a double-Hertz model. *J. Mech. Phys. Solids* 61, 2473–2492.
- Ke, L.L., Wang, Y.S., 2006. Two-dimensional contact mechanics of functionally graded materials with arbitrary spatial variations of material properties. *Int. J. Solids Struct.* 43, 5779–5798.
- Ke, L.L., Yang, J., Kitipornchai, S., Wang, Y.S., 2008. Electro-mechanical frictionless contact behavior of a functionally graded piezoelectric layered half-plane under a rigid punch. *Int. J. Solids Struct.* 45, 3313–3333.
- Lanzoni, L., 2011. Analysis of stress singularities in thin coatings bonded to a semi-infinite elastic substrate. *Int. J. Solids Struct.* 48, 1915–1926.
- Lanzoni, L., Radi, E., 2009. Thermally induced deformations in a partially coated elastic layer. *Int. J. Solids Struct.* 46, 1402–1412.
- Lanzoni, L., Radi, E., 2016. A loaded Timoshenko beam bonded to an elastic half plane. *Int. J. Solids Struct.* 92–93, 76–90.
- Qian, Z., Jin, F., Lu, T., Kishimoto, K., 2009. Transverse surface waves in a layered structure with a functionally graded piezoelectric substrate and a hard dielectric layer. *Ultrasonics* 49, 293–297.
- Shield, T.W., Kim, K.S., 1992. Beam theory models for thin film segments cohesively bonded to an elastic half space. *Int. J. Solids Struct.* 29, 1085–1103.
- Suresh, S., 2001. Graded materials for resistance to contact deformation and damage. *Science* 292, 2447–2451.
- Suresh, S., Giannakopoulos, A.E., Alcalá, J., 1997. Spherical indentation of compositionally graded materials: Theory and experiments. *Acta Mater.* 45, 3087–3087.
- Yu, H.H., He, M.Y., Hutchinson, J.W., 2001. Edge effects in thin film delamination. *Acta Mater.* 49, 93–107.